

Analytical solution of the Schrödinger equation with $1/r^3$ and attractive $1/r^2$ potentials: Universal three-body parameter of mixed-dimensional Efimov states

Yuki Ohishi,^{1,*} Kazuki Oi,^{2,1,*} and Shimpei Endo^{1,3}

¹*Department of Engineering Science, University of Electro-Communications, Chofu, Tokyo 182-8585, Japan*

²*Department of Physics, Tohoku University, Sendai 980-8578, Japan*

³*Institute for Advanced Science, University of Electro-Communications, Chofu, Tokyo 182-8585, Japan*

(Dated: January 28, 2026)

We study the Schrödinger equation with $1/r^3$ and attractive $1/r^2$ potentials. Using the quantum defect theory, we obtain analytical solutions for both repulsive and attractive $1/r^3$ interactions. The obtained discrete-scale-invariant energies and wave functions, validated by excellent agreement with numerical results, provide a natural framework for describing the universality of Efimov states in mixed dimension. Specifically, we consider a three-body system consisting of two heavy particles with large dipole moments confined to a quasi-one-dimensional geometry and resonantly interacting with an unconfined light particle. With the Born-Oppenheimer approximation, this system is effectively reduced to the Schrödinger equation with $1/r^3$ and $1/r^2$ potentials, and manifests the Efimov effect. Our analytical solution suggests that, for repulsive dipole interactions, the three-body parameter of the mixed-dimensional Efimov states is universally set by the dipolar length scale, whereas for attractive interactions it explicitly depends on the short-range phase. We also investigate the effects of finite transverse confinement and find that our analytical results are useful for describing the Efimov states composed of two polar molecules and a light atom.

I. INTRODUCTION

Cold atoms and molecules have recently emerged as versatile platforms for exploring a wide range of quantum phenomena [1–3]. Owing to their high degree of controllability, cold-atom systems have enabled the realization of various exotic effects that are unique to strongly interacting quantum matters. A prime example of such exotic few-body phenomena is the Efimov effect [4–9]: a series of three-body bound states exhibiting discrete scale invariance emerges when the s -wave scattering lengths characterizing the strength of short-range interactions are resonantly enhanced via a Feshbach resonance [10, 11]. As the Efimov states can appear in various physical systems such as ${}^4\text{He}$ cluster [12, 13], condensed matters [14], to nuclear physics [15–20], they have been explored in cold-atom experiments to unveil their universal nature [4, 21–25].

More recently, cold atoms and molecules with a long-range $1/r^3$ interaction have been established as platforms for exploring even more exotic quantum phenomena [26, 27], such as the supersolid phase [28–30], Einstein de Haas effect [31, 32], quantum magnetism [33–35], and controlled chemical reactions [36–39]. In addition to serving as platforms for quantum many-body simulations, polar molecules - owing to their long-range interactions and the suppression of inelastic losses via microwave shielding [40, 41] - have also been recognized as promising candidates for quantum computation [3, 42, 43]. To obtain a detailed account of the exotic quantum phenomena induced by long-range dipolar interactions and to achieve quantum computation with molecules, a microscopic un-

derstanding of the underlying two- and three-body processes is crucial.

Because the dipole–dipole interaction scales as $1/r^3$ at large distance, its low-energy few-body scattering properties differ markedly from those of short-range interactions [44, 45]. For the two-body system, the effective range expansion, which is widely used in cold-atom studies, breaks down owing to the peculiar threshold behavior, giving rise to a distinct class of universality characterized by the dipole length scale [46–48]. This anomalous two-body scattering property strongly influences three- and many-body physics. Indeed, the Efimov states with dipolar interactions have been demonstrated to depend universally on the dipole length scale [49, 50], in stark contrast to systems of shorter-range $1/r^6$ van der Waals interactions, where the Efimov states are universally determined by the van der Waals length [51–57].

To obtain a quantitatively better understanding of few- and many-body quantum systems based on accurate two-body correlations, analytical solutions of the Schrödinger equation with $1/r^n$ potentials are highly valuable. After Gao analytically solved the Schrödinger equation with an attractive $1/r^6$ potential using the quantum defect theory and its low-energy expansion [58–60], a series of analytical solutions has been derived for various classes of $1/r^n$ interactions: $1/r^3$ potential [47, 61, 62], general $1/r^n$ ($n > 2$) potentials [61], repulsive $1/r^6$ potential [63], harmonically trapped system [64], an anisotropic $1/r^3$ potential [65], and multi-channel systems [66, 67]. The method has further been extended to systems involving both attractive $1/r^6$ and $1/r^2$ potentials [68] to investigate the Efimov physics, revealing the van der Waals universality of Efimov states by deriving analytical expressions for their binding energies and wave functions.

Here, we obtain analytical solutions of the Schrödinger equation with $1/r^3$ and attractive $1/r^2$ potentials us-

* These authors contributed equally to this work.

ing the quantum defect theory. For a repulsive $1/r^3$ potential, the binding energies and wave functions are independent of short-range physics and are universally determined by the length scale of $1/r^3$ interaction. In contrast, for an attractive $1/r^3$ potential, our analytical expressions explicitly depend on short-range physics through the quantum defect parameter. These analytical solutions are valuable for describing Efimov states appearing in mixed-dimensional geometries [69, 70]. To illustrate this point, we apply our analytical solutions to a three-body system composed of two heavy dipolar particles confined in a tight cigar-shaped trap and interacting with a light particle with a large s -wave scattering length, which leads to the Born-Oppenheimer equation of the form of the Schrödinger equation with $1/r^3$ and attractive $1/r^2$ potentials. Our analytical solutions provide explicit formulae of the three-body parameters of the mixed-dimensional Efimov states, revealing that the nature of universality differs between repulsive and attractive $1/r^3$ interactions. We show that our analytical solutions can well describe the behavior of polar molecules [26, 36–41, 71, 72] confined in a tight cigar-shaped trap, whereas the influence of the transverse trapping potential is non-negligible in the case of dipolar atoms [73–75].

This paper is organized as follows. In Sec. II, we first explain how the $1/r^2$ and $1/r^3$ potentials arise in mixed-dimensional systems of atoms and molecules with dipole-dipole interactions, and then present the analytical solutions of the corresponding Schrödinger equation at the unitary limit. In Sec. III, we compare the analytical solutions with the numerical results and discuss the experimental feasibility of realizing our system, including discussions on the effect of the transverse trapping potential. Finally, we summarize our findings in Sec. IV. Throughout this paper, we use natural units with $\hbar = 1$.

II. ANALYTICAL SOLUTION WITH $1/r^3$ AND $1/r^2$ POTENTIALS AND EFIMOV PHYSICS WITH DIPOLE INTERACTION IN MIXED DIMENSION

In this section, we present the analytical solutions of the Schrödinger equation under $1/r^2$ and $1/r^3$ potentials

$$\left[-\frac{1}{2\mu} \frac{d^2}{dr^2} + \frac{s^2 - \frac{1}{4}}{2\mu r^2} - \frac{C_3}{r^3} \right] \psi(r) = E\psi(r), \quad (1)$$

where μ is the reduced mass, and C_3 is the strength of repulsive ($C_3 < 0$) and attractive ($C_3 > 0$) $1/r^3$ interaction, whose characteristic length scale can be defined as $\beta_3 = 2\mu|C_3|$. s^2 is a constant characterizing the strength of the $1/r^2$ potential. For integer values of angular momenta $\ell = 0, 1, 2, \dots$ with $s^2 = (\ell + 1/2)^2 > 0$, Eq. (1) has been solved analytically with the quantum defect theory (QDT) [47, 59–62, 65, 68]. As we show in detail in Sections II A and II B, this equation can also be solved

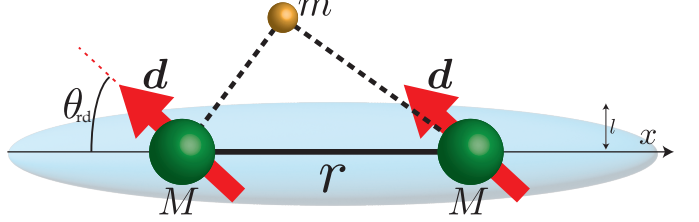


FIG. 1. Schematic illustration of the three-body system studied in Eq. (2): we consider a system two heavy particles (mass M) with dipole moments \mathbf{d} interacting with a light particle (mass m) with an s -wave scattering length $a^{(\text{HL})}$ (black dotted line). The heavy particles are assumed to be confined in an axially symmetric harmonic trap (trapping length l), while the light particle move freely in a three dimensional space. The direction of the dipole moment θ_{rd} can be controlled by an external field.

analytically for arbitrary negative values $s^2 < 0$ (i.e., a pure imaginary s).

Equation (1) with $s^2 < 0$ is relevant to Efimov states of cold atoms and molecules interacting with dipole-dipole interactions in a mixed dimension. To illustrate this point, we consider a three-body system composed of two heavy particles (mass M) and a light particle (mass m) as illustrated in Fig. 1. We consider a mixed dimensional system [69, 70], such that the heavy particles are confined by an axially symmetric harmonic trap (see Eq. (3)) while the light particle moves freely in a three-dimensional space. The heavy particles are assumed to possess large dipole moments, such that they interact predominantly via a dipole-dipole interaction at large distance. Such a system can be realized with highly magnetic cold atoms, such as Cr [73], Er [74], and Dy [75], or with polar molecule [26, 36–41, 71, 72]. On the other hand, the light particle is assumed to have a negligibly small dipole moment, so that the interaction between the light and heavy particles is of the short-range van der Waals type. We model this short-range interaction between the heavy and light particles by a zero-range contact interaction characterized by the s -wave scattering length $a^{(\text{HL})}$ [76]. This assumption is particularly appropriate for describing low-energy bound and scattering states of cold atoms and molecules [11].

When the mass ratio between the heavy and light particle is large $M/m \gg 1$, the system can be well described by the Born-Oppenheimer approximation, where the effect of the light particle is incorporated as an effective interaction between the heavy particles. The Schrödinger equation for the relative motion of the two-heavy particles (dipole moments \mathbf{d}) is written as

$$\left[-\frac{\nabla^2}{M} + V_{\text{BO}}(\mathbf{r}) + V_{\text{dd}}(\mathbf{r}) + V_{\text{HO}}(\mathbf{r}) \right] \phi(\mathbf{r}) = E\phi(\mathbf{r}). \quad (2)$$

Here, V_{HO} is an axially symmetric external harmonic po-

tential acting solely on the heavy particles

$$V_{\text{HO}}(\mathbf{r}) = \frac{M}{2} \omega^2 (y^2 + z^2) \quad (3)$$

with the transverse trapping frequencies ω , and V_{dd} is the dipole-dipole interaction between the heavy particles

$$V_{\text{dd}}(\mathbf{r}) = \frac{C_{\text{dd}}(1 - 3 \cos^2 \theta_{\text{rd}})}{r^3}, \quad (4)$$

where C_{dd} denotes the dipole-dipole coupling constant and θ_{rd} is the angle between \mathbf{r} and \mathbf{d} . $V_{\text{BO}}(r)$ is the Born-Oppenheimer potential originating from the exchange of the light particle, which is analytically obtained as [77]

$$V_{\text{BO}}(r) = -\frac{1}{2mr^2} \left(\frac{r}{a^{(\text{HL})}} + W \left(e^{-\frac{r}{a^{(\text{HL})}}} \right) \right)^2 \Theta \left(\frac{r}{a^{(\text{HL})}} + 1 \right), \quad (5)$$

where W and Θ are the Lambert W function and the Heaviside step function, respectively.

When the transverse trapping frequency is large, the heavy particles can be considered to remain in the transverse ground state. For such a tight cigar-shaped trap, integrating $V_{\text{dd}}(\mathbf{r})$ over the transverse directions (y and z) with the transversal ground-state wave function yields a one-dimensional Schrödinger equation ($\psi(r) = r\phi(r)$)

$$\left[-\frac{1}{M} \frac{d^2}{dr^2} + V_{\text{BO}}(r) + V_{\text{q1D}}(r) \right] \psi(r) = E\psi(r) \quad (6)$$

with an effective quasi-one-dimensional dipole-dipole interaction [78, 79]

$$V_{\text{q1D}}(r) = -\frac{C_{\text{dd}}[1 + 3 \cos 2\theta]}{8l^3} v(r/l), \quad (7)$$

with

$$v(x) = -2x + \sqrt{2\pi} (1 + x^2) e^{\frac{x^2}{2}} \text{erfc}(x/\sqrt{2}). \quad (8)$$

Here, $l = \sqrt{\hbar/M\omega}$ is the harmonic oscillator length of the transverse confinement, and $\theta = \theta_{\text{rd}}$ is the angle between the axial direction and \mathbf{d} .

In the unitary limit $a^{(\text{HL})} \rightarrow \pm\infty$, the Born-Oppenheimer potential reduces to $V_{\text{BO}}(r) \sim 1/r^2$. Furthermore, considering the limit of a tight cigar-shaped trap $\omega \rightarrow \infty$, the effective potential reduces to $V_{\text{q1D}}(r) \sim 1/r^3$. We thus obtain Eq. (1) with $\mu = M/2$ and

$$s^2 = \frac{1}{4} - \frac{M\Omega^2}{2m}, \quad (9)$$

where $\Omega = W(1) = 0.5671\dots$, and

$$C_3 = C_{\text{dd}}(1 + 3 \cos 2\theta)/2. \quad (10)$$

Due to the $1/r^2$ attraction ($s^2 < 0$), it shows the Efimov effect [69]. The analytical solutions of Eq. (1), derived in Sec. II A and II B, are thus relevant for the Efimov physics of dipolar atoms or polar molecules in a mixed dimension. Such a system can be experimentally realized

by a mixture of light cold atoms with heavy cold dipolar atoms or polar molecules selectively confined in an optical lattice, with the heavy-light interaction fine-tuned as $a^{(\text{HL})} \rightarrow \pm\infty$ by the Feshbach resonance [80–86]. Notably, by varying the direction of the external magnetic or electric fields, the direction of the dipole moment \mathbf{d} hence the strength of $1/r^3$ interaction C_3 can be controlled to realize either repulsive $C_3 < 0$ or attractive $C_3 > 0$ interactions [36, 37, 73–75, 87].

A. Repulsive $1/r^3$ and attractive $1/r^2$ potentials

The analytical solutions of Eq. (1) can be obtained in a similar manner to that employed in Ref. [68]: By generalizing Gao's quantum defect theory (QDT) [62] to the case of $s^2 < 0$, a general solution of Eq. (1) is expressed as a linear combination of the two independent special solutions $f^c(r)$ and $g^c(r)$ as (see Eq. (A1) in the Appendix for concrete expressions of f^c and g^c)

$$\psi(r) = \mathcal{N}[f^c(r) - K^c g^c(r)], \quad (11)$$

where K^c is the QDT parameter which characterizes the phase shift at short-range region $r \ll \beta_3$ and \mathcal{N} is a normalization constant.

For bound states, the solution must satisfy the boundary condition $\psi(r \rightarrow \infty) = 0$, from which we obtain

$$K^c = \frac{W_{f-}}{W_{g-}} = \frac{1}{\sin[2\pi(\nu - \nu_0)]} \frac{1 - \mathcal{M}}{1 + \mathcal{M}}, \quad (12)$$

where $\nu_0 = s = i|s|$, W_{f-} and W_{g-} are given as Eqs. (32) and (34) in Ref. [62], and \mathcal{M} defined as in Eq. (A16) can be evaluated at low energy $|\Delta| \ll 1$ (with $\Delta \equiv \sqrt{2\mu E \beta_3}/2$) as

$$\mathcal{M} \approx |\Delta|^{2\nu_0} \frac{\Gamma(1 - 2\nu_0)}{\Gamma(1 + \nu_0)} \frac{\Gamma(1 - \nu_0)}{\Gamma(1 + 2\nu_0)}. \quad (13)$$

In the absence of the Efimov effect, ν_0 is real, and thus $\mathcal{M} \simeq 0$ in the low-energy limit $|\Delta| \rightarrow 0$. Indeed, the binding energy and low-energy scattering parameters for a two-body problem with a $1/r^3$ potential in the ℓ -th angular momentum channel can be obtained from Eqs. (12) and (13) by setting $\nu_0 = 2\ell+1$ [47, 62]. In contrast, when the system has an attractive $1/r^2$ potential with $s^2 < 0$ as in Eq. (1), ν_0 becomes pure imaginary $\nu_0 = i|s|$. Consequently, the behavior of \mathcal{M} at low energy $|\Delta| \rightarrow 0$ is modified as

$$\mathcal{M} \cong -e^{i\{2|s|\log|\Delta| - 2\xi\}}, \quad (14)$$

where

$$\xi \equiv \arg[\Gamma(i|s|)\Gamma(1 + 2i|s|)]. \quad (15)$$

The log-periodic behavior of Eq. (14) as a function of energy $\Delta = \sqrt{2\mu E \beta_3}/2$ is a clear manifestation of the discrete-scale invariance of the Efimov effect.

As shown in the Appendix (see Eq. (A12)), f^c decreases exponentially as $r \rightarrow 0$ while g^c increases exponentially, corresponding to a regular and irregular solution, respectively. If the length scale associated with the short-range physics R_{\min} is small $R_{\min} \ll \beta_3$, as is the case for cold atoms and molecules, the wave function should be solely described by the regular solution f^c . In other words, the wave function in the short-range region $r \ll \beta_3$ should be suppressed due to the repulsive $1/r^3$ potential, which results in $K^c \cong 0$, or equivalently, $\mathcal{M} \cong 1$. Substituting this into Eq. (14), we obtain an analytical expression of the three-body binding energy as

$$E_n = -\frac{2}{\mu\beta_3^2} \exp\left(\frac{\pi}{|s|} + \frac{2}{|s|}\xi\right) \times e^{-\frac{2n\pi}{|s|}}, \quad (16)$$

where n is an integer quantum number characterizing the n -th Efimov states. The discrete-scale invariance with a scale factor $e^{2\pi/|s|}$ naturally emerges as an analytical continuation: by converting a real value $\nu_0 = 2\ell+1$ corresponding to a centrifugal repulsion into a pure imaginary value $\nu_0 = s = i|s|$ corresponding an Efimov attraction, the low-energy behavior of \mathcal{M} in Eq. (13) leads to the discrete-scale-invariant energy spectrum. Equation (16) can therefore be regarded as an analytical continuation of the binding-energy formula for a two-body problem with a $1/r^3$ repulsion and a centrifugal barrier obtained in Refs. [47, 62].

Notably, the binding energy in Eq. (16) is independent of the QDT parameter K^c and the short-range boundary condition R_{\min} . In other words, the three-body parameter of the Efimov states is universally determined by β_3 characterizing the long-range dipole potential $1/r^3$. This universality arises from the suppression of the wave function at short distance caused by the $1/r^3$ repulsion. It is analogous to the universality found for three identical dipolar bosons in Ref. [49]. While a hyperspherical repulsive potential arising from the coupling of multiple angular-momentum channels is required to describe the three identical dipoles [49], our mass-imbalanced mixed-dimensional system allows a simple analytical description of the dipolar Efimov universality, which shares common underlying mechanism — a repulsive potential at the scale $\simeq \beta_3$ — as the physical origin of the universality. As another notable analogous system, for three identical bosons interacting via van der Waals forces, the three-body parameter has been found both experimentally [51, 52, 88–91] and theoretically [53–55, 92–97] to be universally determined by the van der Waals length for broad Feshbach resonances. In this system, the non-adiabatic repulsion appearing universally at the van der Waals scale is demonstrated to suppress short-range configurations, leading to a universal three-body parameter [53–55].

While the solutions f^c , g^c and hence the bound-state wave function at finite binding energy is represented as a complicated Bessel series expansion (see Appendix), they can be expressed simpler at low energy (or equivalently,

at short distance) $r \ll 1/\sqrt{2\mu|E|}$ as

$$\begin{aligned} f^c(r) &= -\frac{2}{\sinh(2\pi|s|)} \operatorname{Im} \left[\sqrt{r} I_{2i|s|} \left(2\sqrt{\frac{\beta_3}{r}} \right) \right], \\ g^c(r) &= -2\operatorname{Re} \left[\sqrt{r} I_{2i|s|} \left(2\sqrt{\frac{\beta_3}{r}} \right) \right]. \end{aligned} \quad (17)$$

The regular and irregular behavior of f^c, g^c at short distance [Eq. (A12)] can also be understood from these expressions, as an asymptotic behavior of the modified Bessel function I with a pure imaginary index.

B. Attractive $1/r^3$ and attractive $1/r^2$ potentials

The analytical solution for an attractive potential $C_3 > 0$ is obtained with a procedure similar to that in the repulsive case. The two independent special solutions $f^c(r)$ and $g^c(r)$ are given as Eq. (A27), which is similar but slightly different from the repulsive case in Eq. (A1). Using these two solutions, a general solution is expressed by the same formula as Eq. (11). The bound-state condition is obtained by imposing the boundary condition $\psi(r \rightarrow \infty) = 0$ as

$$K^c = \frac{W_{f-}}{W_{g-}} = \tan(\nu\pi) \frac{1 + \mathcal{M}}{1 - \mathcal{M}}, \quad (18)$$

where W_{f-} and W_{g-} are given as Eq. (A31), and the definition of \mathcal{M} is same as in the repulsive case.

One notable difference from the repulsive case is that both f^c and g^c are of the same order at short distance and contribute equally to the wave function, allowing K^c to take an arbitrary value. In other words, the binding energy can explicitly depend on K^c , hence short-range phase. To be more specific, by using the low-energy expansion formula Eq. (14) and $\nu \simeq s = i|s|$, Eq. (18) is written as

$$K^c \cong \tanh(\pi|s|) \tan \left[\frac{|s|}{2} \log |\Delta| - \xi \right], \quad (19)$$

from which the three-body binding energy is obtained as

$$E_n = -\frac{2}{\mu\beta_3^2} \exp\left(\frac{2}{|s|} \left[\arctan\left(\frac{K^c}{\tanh(\pi|s|)}\right) + \xi \right]\right) \times e^{-\frac{2n\pi}{|s|}}. \quad (20)$$

The discrete-scale invariance of the Efimov states thus naturally emerges as an analytical continuation of the two-body solution under an attractive $1/r^3$ potential and a centrifugal barrier [47, 61]. In contrast to the repulsive $1/r^3$ case in Eq. (16), the three-body binding energy explicitly depends on the QDT parameter K^c . This difference can be ascribed to the short-range behavior of the wave function: Due to the attractive potential $1/r^3$, the wave function can penetrate into the short-range region $r \ll \beta_3$, causing the binding energy to depend explicitly on the short-range detail through K^c . To further elucidate this point, we note that at short distance

$r \ll 1/\sqrt{2\mu|E|}$, the solutions f^c, g^c have simpler analytical expressions [61],

$$\begin{aligned} f^c(r) &= \frac{1}{\cosh(\pi|s|)} \operatorname{Re} \left[\sqrt{r} J_{2i|s|} \left(2\sqrt{\frac{\beta_3}{r}} \right) \right], \\ g^c(r) &= -\frac{1}{\sinh(\pi|s|)} \operatorname{Im} \left[\sqrt{r} J_{2i|s|} \left(2\sqrt{\frac{\beta_3}{r}} \right) \right]. \end{aligned} \quad (21)$$

In contrast to the repulsive case in Eq. (17), both f^c and g^c oscillate rapidly at short distance and their magnitudes are of the same order [see Eq. (A30)]. Substituting Eq. (21) into the hard-wall boundary condition $\psi(r = R_{\min}) = 0$, the QDT parameter K^c is related to R_{\min} as

$$K^c = -\tanh(\pi|s|) \frac{\operatorname{Re} \left[J_{2i|s|} \left(2\sqrt{\frac{\beta_3}{R_{\min}}} \right) \right]}{\operatorname{Im} \left[J_{2i|s|} \left(2\sqrt{\frac{\beta_3}{R_{\min}}} \right) \right]} \quad (22)$$

$$\cong -\frac{1}{\tan \left[2\sqrt{\frac{\beta_3}{R_{\min}}} - \frac{\pi}{4} \right]}. \quad (23)$$

In the last line, we use the asymptotic form of the Bessel function. This equation demonstrates that the QDT parameter K^c depends on the short-range physics through R_{\min} which incorporates the phase shift acquired by a complicated short-range potential not captured by $V_{dd}(\mathbf{r})$.

While the explicit dependence of the binding energy in Eq. (20) on K^c appears to indicate a nonuniversal sensitivity of the Efimov state to short-range details of the atoms, such as electronic structures and internal spins, we stress that it may still be cast in a universal description by employing a low-energy scattering parameter of the two heavy particles. To elucidate this point, let us neglect the presence of the light particle and consider two heavy particles in the same confined geometry, whose Schrödinger equation is given by Eq. (1) with $s = 1/2$. Although this two-body Schrödinger equation differs from the three-body Efimovian system of Eq. (1) with $s^2 < 0$ for $r \gtrsim \beta_3$, the short-range behavior at $r \ll \beta_3$ are the same, as reflected in the s -independence in Eq. (23) (see also the leading order term of Eq. (A30) in the Appendix). Since the low-energy two-body scattering parameter such as the scattering length is universally related to K^c [47, 61], Eq. (20) can be rewritten as its universal function. This universality is analogous to the van der Waals universality in highly mass-imbalanced systems, where the universal relation between K^c and the s -wave scattering length $a^{(HH)}$ of the heavy particles result in a universal three-body parameter determined by the van der Waals length and $a^{(HH)}$ [56, 57, 68, 98]. From this perspective, the K^c -independent result for the repulsive $1/r^3$ potential in Eq. (16) can be alternatively interpreted as a case where the low-energy scattering parameter and K^c are universally determined by the dipole length β_3 [46–48], so that the Efimov states are universally determined by β_3 . In the above argument, as well

as in Ref. [68], it is implicitly assumed that the short-range three-body phase is dominated by the short-range interaction between the heavy particles, and the contribution from the light particle can be neglected. This assumption is particularly valid for highly mass-imbalanced heavy-heavy-light atomic or molecular systems, where the polarizability of the light particle is relatively small and hence its short-range van der Waals and higher-order forces are correspondingly weaker than those of the heavy particles.

III. COMPARISON WITH NUMERICAL RESULTS

In this section, we present our numerical solutions of Eqs. (1) and (6), and compare them with the analytical solutions derived in Sec. II. Equations (1) and (6) are solved numerically by imposing the fixed boundary conditions at relatively short and sufficiently large distances: $\psi(r = R_{\min}) = 0$ and $\psi(r = R_{\max}) = 0$ with $R_{\min} \ll \beta_3 \ll R_{\max}$. We discretize the radial coordinate between R_{\min} and R_{\max} using an exponential grid. The calculations are performed with a grid of 5000-10000 points ranging with $R_{\max}/R_{\min} = 1000 - 2000$. With these parameters, the numerical relative error is confirmed to be of order 10^{-5} - 10^{-6} . Given our specific interest to dipolar atoms and polar molecules, we perform the calculations for the mass ratios corresponding to ^{167}Er - ^6Li atoms ($M/m = 27.7520\dots$), and ^6Li atom and ^{23}Na - ^{40}K molecule ($M/m = 10.4659\dots$), respectively.

A. One-dimensional limit

In Fig. 2(a), we show the numerical solution of Eq. (1) with a repulsive $1/r^3$ potential $C_3 < 0$ at the unitary limit $1/a^{(\text{HL})} = 0$. The discrete-scale-invariant energy spectra obtained numerically agree excellently with the analytical expression (solid lines) in Eq. (16) with $\mu = M/2$ for $\beta_3/R_{\min} \gtrsim 5$. This demonstrates that the three-body parameter of the Efimov states is insensitive to R_{\min} and is instead universally determined by the dipole interaction length scale β_3 , due to a strong repulsive potential that prevents the particles from getting close. This feature is also evident in the behavior of the wave function shown in Fig. 3: the wave function is exponentially suppressed at short distances, in agreement with the analytical expression for $r \ll 1/\sqrt{M|E|}$ in Eq. (17) (dashed curves) [see also the leading order term of Eq. (A12)].

For a loosely bound state of $M\beta_3^2|E| \lesssim 10^{-2}$ and $\beta_3/R_{\min} \gtrsim 50$ in Fig. 2(a), the finite-size effect in our numerical calculation of $R_{\max}/R_{\min} = 2000$ is visible as the spatial extent of the bound state becomes comparable to the system size R_{\max} . On the other hand, the discrepancy for $\beta_3/R_{\min} \lesssim 5$ in Fig. 2(a) originates from the breakdown of the condition $\beta_3/R_{\min} \gg 1$ used in deriving

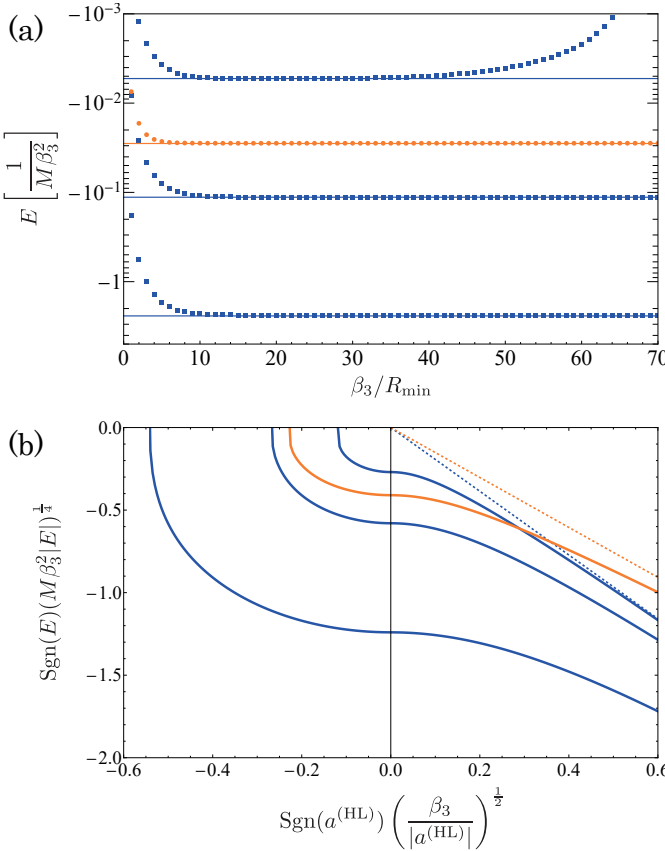


FIG. 2. (a) Energy spectra of the Efimov bound states under a repulsive $1/r^3$ potential at the unitary limit $1/a^{(\text{HL})} = 0$ calculated with $R_{\text{max}}/R_{\text{min}} = 2000$. Blue squares (orange circles) show the energies obtained by numerically solving Eq. (1) for mass ratios corresponding to ^{167}Er - ^6Li atoms $M/m = 27.7520\dots$ (^6Li atom and ^{23}Na - ^{40}K molecule $M/m = 10.4659\dots$), respectively. Solid curves denote the analytical result in Eq. (16) with $\mu = M/2$. (b) Energy spectra for finite heavy-light s -wave scattering length $a^{(\text{HL})}$, calculated with $\beta_3/R_{\text{min}} = 16.0$. We only show three and one states among the whole Efimov series for ^{167}Er - ^6Li (blue) and ^{23}Na - ^{40}K - ^6Li (orange), respectively. Dashed lines denote the heavy-light dimer states, into which the Efimov trimers dissociate for $a^{(\text{HL})} \rightarrow +0$.

Eq. (16). Indeed, in the limit of $\beta_3/R_{\text{min}} \rightarrow 0$, the binding energy of the Efimov states becomes $E \propto 1/M R_{\text{min}}^2$, which is distinct from $E \propto 1/M \beta_3^2$ of Eq. (16). The energy spectra away from the unitary limit $1/a^{(\text{HL})} \neq 0$ are shown in Fig. 2(b). The discrete-invariant spectra of the Efimov states are clearly demonstrated, together with the Borromean character for $a^{(\text{HL})} < 0$ and particle-dimer dissociation for $a^{(\text{HL})} > 0$ [5–9]. We confirm that the results obtained for different values of β_3/R_{min} collapse excellently onto the same curves, demonstrating the universality, with a small noticeable deviation for the most tightly bound Efimov state in Fig. 2(b). Although we also find deeply bound trimers of $M\beta_3^2|E| \gtrsim 100$ (not shown in Fig. 2(a) and (b)), these states do not exhibit discrete-

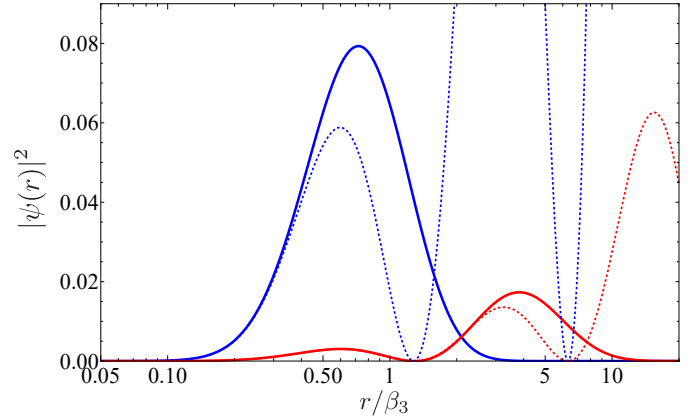


FIG. 3. Efimov states' wave function for a repulsive $1/r^3$ potential, obtained by solving Eq. (1) with $M/m = 27.7520\dots$, $R_{\text{min}}/\beta_3 = 0.05$, and $R_{\text{max}}/\beta_3 = 20.0$. Blue (red) solid curves are the ground and first-excited Efimov states, respectively. Dashed curves denote analytical solutions for $r \ll 1/\sqrt{M|E|}$ in Eqs. (17) and (11) with $K^c = f^c(R_{\text{min}})/g^c(R_{\text{min}})$.

scale invariance or universality. We therefore identify the trimer with $M\beta_3^2|E| \sim 1$ as the ground Efimov trimer.

In Fig. 4(a), we show the numerical solution of Eq. (1) with an attractive $1/r^3$ potential $C_3 > 0$ at the unitary limit $1/a^{(\text{HL})} = 0$. They agree excellently with the analytical expression (solid curves) in Eqs. (20) and (22). In contrast to the repulsive case, the energy spectra depend on β_3/R_{min} through the quantum defect parameter K^c , as described by the universal formula in Eq. (20). This is consistent with behavior of the wave function shown in Fig. 5: unlike the repulsive case, the wave function exhibits rapid oscillations and penetrates into the short-distance region, in agreement with the analytical expression for $r \ll 1/\sqrt{M|E|}$ in Eq. (21) (dashed curves) [see also the leading order term of Eq. (A30)]. A discrepancy for $M\beta_3^2|E| \lesssim 10^{-2}$ and $\beta_3/R_{\text{min}} \gtrsim 50$ in Fig. 4(a) is due to the finite-size effect of the trimer becoming similar size as the large-distance boundary. On the other hand, a discrepancy for deeply bound states $M\beta_3^2|E| \gtrsim 10$ is due to the breakdown of the low-energy condition $M\beta_3^2|E| \ll 1$ used in deriving Eq. (20). The energy spectra away from the unitary limit $1/a^{(\text{HL})} \neq 0$ are shown in Fig. 4(b). While different β_3/R_{min} generally yield different values of K^c hence different spectra, they are confirmed to collapse almost perfectly onto the same universal curves when the corresponding K^c value (i.e., the three-body short-range phase) is identical, with a small noticeable deviation for the ground Efimov state.

B. Effect of axial harmonic confinement

In this section, we study the effect of an axially symmetric harmonic confinement according to Eq. (6). By comparing the results of one-dimensional limit $\omega \rightarrow \infty$ in Secs. II A and II B with those for finite ω in Eq. (6),

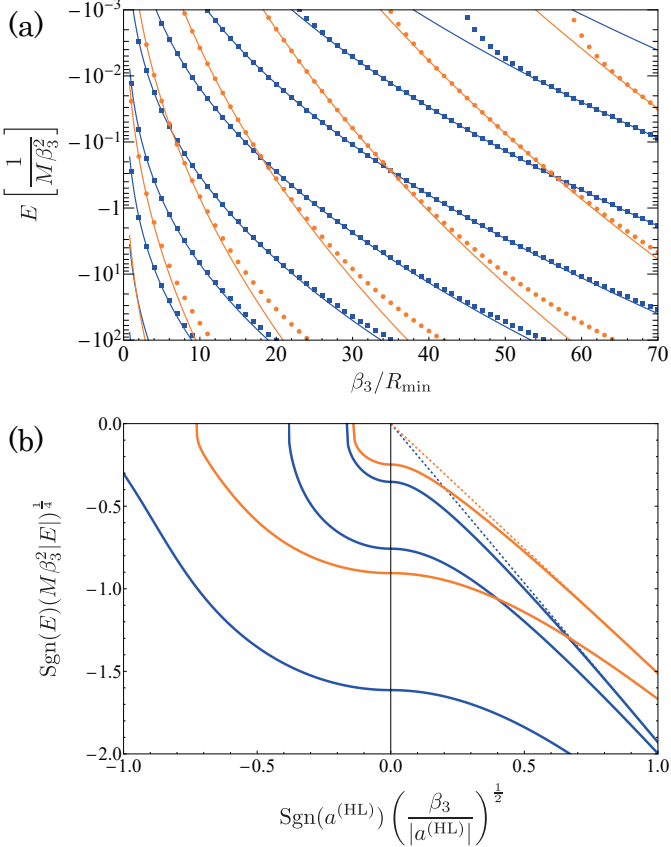


FIG. 4. (a) Energy spectra of the Efimov bound states under an attractive $1/r^3$ potential at the unitary limit $1/a^{(\text{HL})} = 0$. Solid curves denote the analytical result in Eqs. (20) and (22) with $\mu = M/2$. (b) Energy spectra for finite heavy-light s -wave scattering length $a^{(\text{HL})}$, obtained with $\beta_3/R_{\min} = 10.0$. We only show three and two states among the whole Efimov series for ^{167}Er - ^6Li (blue) and ^{23}Na - ^{40}K - ^6Li (orange), respectively.

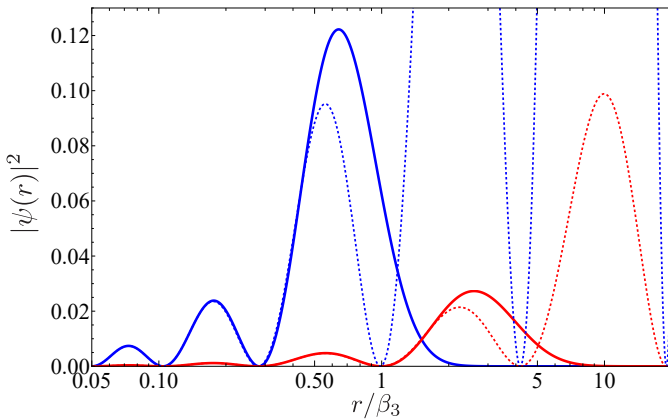


FIG. 5. Efimov states' wave function for an attractive $1/r^3$ potential, obtained by solving Eq. (1) with $M/m = 27.7520\ldots$, $R_{\min}/\beta_3 = 0.05$, and $R_{\max}/\beta_3 = 20.0$. Blue (red) solid curves are the ground and first-excited Efimov states, respectively. Dashed curves denote analytical solutions for $r \ll 1/\sqrt{M|E|}$ in Eqs. (21) and (11) with $K^c = f^c(R_{\min})/g^c(R_{\min})$.

we investigate the extent to which our analytical solutions in Secs. II A and II B are useful for describing the Efimov states of dipolar atoms or polar molecules in a mixed dimension.

In Fig. 6, we show the numerical solution of Eq. (6) with a repulsive $1/r^3$ potential $C_3 < 0$ for variable values of harmonic trapping strength $l = \sqrt{\hbar/M\omega}$ at the unitary limit $1/a^{(\text{HL})} = 0$. For a tight harmonic confinement $l/\beta_3 \ll 1$, the results agree excellently with the analytical expression in Eq. (16) (dotted lines), except for the tightly bound state which does not appear for the ^6Li atom- ^{23}Na - ^{40}K molecule (orange), whose energy $M\beta_3^2|E| \gtrsim 10$ is too large to apply the low-energy analytical expression in Eq. (16). As the trapping strength is weakened, the binding energies increase because of the reduction of the effective dipole repulsion, as the heavy particles can explore three-dimensional configurations and thereby avoid the $1/r^3$ repulsion more efficiently [78, 79]. The discrete-scale invariance with the same scale factor $e^{2\pi/|s|}$ persists even for $l/\beta_3 \gtrsim 1$, as it originates from the common long-range behavior of the potential $V(r) = -(|s|^2 + 1/4)/Mr^2$ at large distance $r \gg \beta_3, l$.

In Fig. 7, we show the results with an attractive $1/r^3$ potential $C_3 > 0$ at the unitary limit $1/a^{(\text{HL})} = 0$. In the tight-trap limit $l/\beta_3 \ll 1$, the results agree excellently with the analytical expression in Eqs. (20) and (22) (dotted lines). Discrepancies for the tightly bound states of $M\beta_3^2|E| \gtrsim 10^2$ in Fig. 7 arises from the breakdown of the low-energy approximation. As the trapping strength is weakened, the binding energies decrease because of the reduction of the effective dipole attraction, as the heavy particles take three-dimensional configurations with less $1/r^3$ attractions [78, 79]. Similar to the repulsive case, the discrete-scale invariance with the same scale factor $e^{2\pi/|s|}$ persists for $l/\beta_3 \gtrsim 1$.

While it is challenging to realize the one-dimensional limit $l/\beta_3 \rightarrow 0$ with dipolar atoms, the condition $l/\beta_3 \ll 1$ is feasible using polar molecules. Indeed, the experimental parameters for the dipolar ^{166}Er atom [27] and the ^{23}Na - ^{40}K polar molecule [72] are estimated, using Eq. (10) and $\theta = 0$ with a typical trapping frequency $\omega/2\pi = 20$ kHz [99, 100], as $l/\beta_3 = 2.6$ and $l/\beta_3 = 0.08$, respectively. As explained in Sec. II [see Eq. (7)], β_3 can be controlled from attractive ($0 \leq \theta < 54.7^\circ$) to repulsive ($\theta > 54.7^\circ$) values by varying the orientation of a static external field. The one-dimensional limits for the repulsive and attractive systems, as well as the crossover between them, are thus within reach of current experimental platforms, such as polar molecules confined in a tightly cigar-shaped trap, or possibly Rydberg atoms [101], which can possess much larger dipole moments.

We note that the quasi-one-dimensional approach used in our work is only applicable to low-energy states. Indeed, it has been demonstrated for two confined dipoles that the quasi-one-dimensional approximation can break down for a distance between two dipoles $r \lesssim l$ [102, 103]. This implies that the results presented in Figs 6 and 7 are

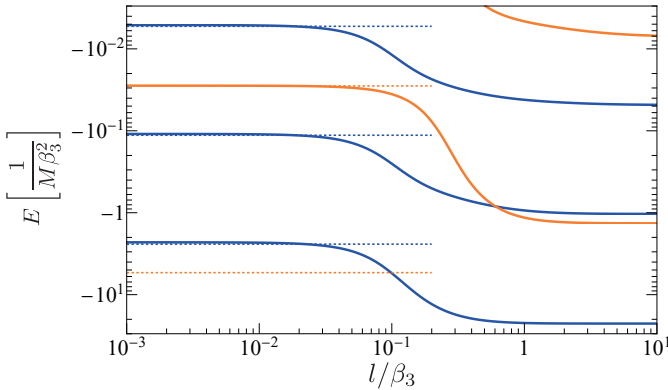


FIG. 6. Energy spectra of the Efimov bound states with a repulsive $1/r^3$ potential under an axially symmetric confinement with a harmonic oscillator length $l = \sqrt{\hbar/M\omega}$, calculated with $R_{\min}/\beta_3 = 0.1$ and $R_{\max}/R_{\min} = 1000$. Blue and orange solid curves show the energies obtained by numerically solving Eq. (1) for mass ratios corresponding to ^{167}Er - ^6Li atoms ($M/m = 27.7520\ldots$), and ^6Li atom and $^{23}\text{Na}^{40}\text{K}$ molecule ($M/m = 10.4659\ldots$), respectively. The dashed lines denote the analytical result in the one-dimensional limit [Eq. (16)].

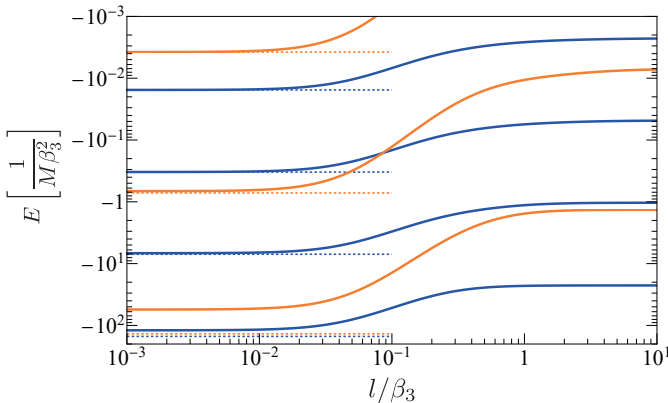


FIG. 7. Energy spectra of the Efimov bound states with an attractive $1/r^3$ potential under an axially symmetric confinement, calculated with $R_{\min}/\beta_3 = 0.1$ and $R_{\max}/R_{\min} = 1000$. Dashed lines denote the analytical result in the one-dimensional limit [Eqs. (20) and (22)].

not be reliable in the right-bottom region $E \lesssim -1/Ml^2$. A three-dimensional treatment, which properly includes excitations into higher transversal modes and resonances induced by them [104], is required to accurately describe those trimers with relatively large binding energies.

IV. CONCLUSION

We have studied the Schrödinger equation with $1/r^3$ and attractive $1/r^2$ potentials and obtained their analytical solutions. By applying the quantum defect theory with complex angular momentum, we have derived the

analytical expressions of the binding energies and wave functions in the low-energy regime for both attractive and repulsive $1/r^3$ potentials, and verified their validity through comparison with numerical solutions. Our work is relevant not only from a mathematical perspective in providing novel analytical solutions of the Schrödinger equation [47, 59–62, 64–66, 68, 98], but also for understanding the physical properties of the Efimov states with long-range interactions. Indeed, the Schrödinger equation with $1/r^3$ and attractive $1/r^2$ potentials naturally arises as the Born–Oppenheimer equation of a three-body system composed of a two heavy particles with large permanent dipole moments confined in a quasi-one-dimensional trap interacting resonantly with an unconfined light particle. Using the analytical solution, we find that the three-body parameter of the mixed-dimensional Efimov states is universally determined by the dipole length for a repulsive system, whereas for an attractive system it explicitly depends on the short-range phase encoded in the quantum defect parameter.

Such mixed-dimensional Efimov states can be realized experimentally using dipolar cold atoms or polar molecules confined in a tight cigar-shaped trap interacting with another atomic species via a Feshbach resonance [80–86]. By investigating the effect of finite transverse confinement, we find that the quasi-one-dimensional analytical solutions are well suited to polar molecules, while the tight-confinement condition is challenging to realize for dipolar atoms. Our findings can thus be tested in experiments with a mixture of polar molecule and a light cold atom by observing enhancements of the three-body loss rate induced by the Efimov states [4, 21–25], under conditions where the two-body losses are efficiently suppressed, for example, by the microwave shielding [40, 41]. They can also be observed through the RF association [105–107], or by the coherent oscillation [108]. More broadly, our analytical solutions provide a useful step toward understanding three-body correlations in strongly correlated quantum many-body systems [109–111].

ACKNOWLEDGMENTS

We thank Peng Zhang and Wenbin Zhong for fruitful discussions. This work was supported by JSPS KAKENHI Grant Numbers JP22K03492, JP23H01174, and JP25K00217. SE acknowledges support from Matsuo Foundation. KO acknowledges support from Graduate Program on Physics for the Universe (GP-PU) of Tohoku University.

Appendix A: Analytical solution with $1/r^3$ and attractive $1/r^2$ potentials

In this Appendix, we present analytical solutions of Eq. (1) for both repulsive and attractive $1/r^3$ potentials.

Our approach is based on the Bessel series expansion supplemented with the quantum defect theory as developed in Refs [47, 59, 61, 62], generalized to the case of an attractive $1/r^2$ potential.

1. Repulsive case

For a repulsive $1/r^3$ potential, Eq. (1) can be solved analytically by generalizing the solutions in Ref. [62] to complex angular momenta as in Ref. [68]. Namely, for a repulsive case, two independent special solutions of Eq. (1) are defined as

$$f^c(r) = \frac{1}{\sin(2\pi\nu)} \left[\frac{\xi(r)}{F(-\nu)} - \frac{\eta(r)}{F(\nu)} \right], \quad (A1)$$

$$g^c(r) = - \left[\frac{\xi(r)}{F(-\nu)} + \frac{\eta(r)}{F(\nu)} \right].$$

Here, $\xi(r)$ and $\eta(r)$ are expressed by expansions of the Bessel function as

$$\xi(r) = \sqrt{r} \sum_{m=-\infty}^{\infty} b_m J_{\nu+m}(x), \quad (A2)$$

$$\eta(r) = \sqrt{r} \sum_{m=-\infty}^{\infty} b_m J_{-\nu-m}(x), \quad (A3)$$

where $x = \sqrt{2\mu E}r$. b_n , $F(\nu)$ are defined in a similar manner to those in Ref. [62] as

$$b_j \equiv \Delta^j \frac{\Gamma(\nu)\Gamma(\nu-\nu_0+1)\Gamma(\nu+\nu_0+1)}{\Gamma(\nu+j)\Gamma(\nu-\nu_0+j+1)\Gamma(\nu+\nu_0+j+1)} c_j(\nu), \quad (A4)$$

$$b_{-j} \equiv \Delta^j \frac{\Gamma(\nu-j+1)\Gamma(\nu-\nu_0-j)\Gamma(\nu+\nu_0-j)}{\Gamma(\nu+1)\Gamma(\nu-\nu_0)\Gamma(\nu+\nu_0)} c_j(-\nu), \quad (A5)$$

$$c_j(\nu) \equiv b_0 Q(\nu) Q(\nu+1) \cdots Q(\nu+j-1), \quad (A6)$$

$$Q(\nu) \equiv \frac{1}{1 - \Delta^2 \frac{Q(\nu+1)}{(\nu+1)[(\nu+1)^2 - \nu_0^2](\nu+2)[(\nu+2)^2 - \nu_0^2]}}, \quad (A7)$$

$$F(\nu) \equiv |\Delta|^{-\nu} \frac{\Gamma(1+\nu_0+\nu)\Gamma(1-\nu_0+\nu)}{\Gamma(1-\nu)} C(\nu), \quad (A8)$$

$$C(\nu) \equiv \lim_{n \rightarrow \infty} c_n, \quad (A9)$$

where $\Delta = \sqrt{2\mu E}\beta_3/2$. In Eqs. (A4) to (A6), j is a positive integer, and the wavefunction is normalized so that $b_0 = 1$. ν is a complex number determined by the transcendental equations [62]

$$(\nu^2 - \nu_0^2) - \frac{\Delta^2}{\nu} [\bar{Q}(\nu) - \bar{Q}(-\nu)] = 0, \quad (A10)$$

where

$$\bar{Q}(\nu) \equiv \{(\nu+1)[(\nu+1)^2 - \nu_0^2]\}^{-1} Q(\nu). \quad (A11)$$

Here, $\nu_0 = s = i|s|$ is pure imaginary. By employing the asymptotic form of the Bessel function, we obtain the asymptotic forms of Eq. (A1) at short distance $r \ll \beta_3$ up to next-to-next-to-leading order as

$$f^c(r) \simeq \sqrt{\frac{r}{\pi}} \left(\frac{r}{\beta_3} \right)^{\frac{1}{4}} \exp \left(-2\sqrt{\frac{\beta_3}{r}} \right) \left[1 - \sqrt{\frac{r}{\beta_3}} \left(|s|^2 + \frac{1}{16} \right) + \frac{r}{2\beta_3} \left(|s|^2 + \frac{9}{16} \right) \left(|s|^2 + \frac{1}{16} \right) \right],$$

$$g^c(r) \simeq -\sqrt{\frac{r}{\pi}} \left(\frac{r}{\beta_3} \right)^{\frac{1}{4}} \exp \left(2\sqrt{\frac{\beta_3}{r}} \right) \left[1 + \sqrt{\frac{r}{\beta_3}} \left(|s|^2 + \frac{1}{16} \right) + \frac{r}{2\beta_3} \left(|s|^2 + \frac{9}{16} \right) \left(|s|^2 + \frac{1}{16} \right) \right]. \quad (A12)$$

On the other hand, the long-range asymptotic forms $r \gg \beta_3$ are obtained as

$$f^c(r) \simeq \frac{1}{\sqrt{2\pi\kappa}} [W_{f-} e^{\kappa r} - W_{f+} (2e^{-\kappa r})], \quad (A13)$$

$$g^c(r) \simeq \frac{1}{\sqrt{2\pi\kappa}} [W_{g-} e^{\kappa r} - W_{g+} (2e^{-\kappa r})],$$

where $\kappa = \sqrt{2\mu|E|}$, and $W_{f\pm}$ and $W_{g\pm}$ are given as Eqs. (32) and (35) in Ref. [62]. Notably, the leading-order term in Eq. (A12) is independent of energy and s , which is an essential requirement for the s -insensitive (i.e. angular-momentum-insensitive) quantum defect theory employed in our work [59].

A general solution for Eq. (1) is expressed using the two independent special solutions as Eq. (11). Therefore, a boundary condition for bound states $\psi(r = \infty) = 0$ is rewritten as

$$K^c = \frac{W_{f-}}{W_{g-}}, \quad (A14)$$

where

$$\frac{W_{f-}}{W_{g-}} = \frac{1}{\sin[2\pi(\nu-\nu_0)]} \frac{1-\mathcal{M}}{1+\mathcal{M}} \quad (A15)$$

with

$$\mathcal{M} \equiv G(-\nu)/G(\nu), \quad (A16)$$

$$G(\nu) \equiv |\Delta|^{-\nu} \frac{\Gamma(1+\nu_0+\nu)\Gamma(1-\nu_0+\nu)}{\Gamma(1-\nu)} C(\nu). \quad (A17)$$

By performing a low-energy expansion, the binding energy can be obtained analytically: at low energy, ν and $C(\nu)$ asymptote as

$$\nu \cong \nu_0, \quad (A18)$$

$$C(\nu) \cong 1. \quad (A19)$$

Therefore, from the definition of $G(\nu)$, \mathcal{M} asymptotes as

$$\begin{aligned} \mathcal{M} &= |\Delta|^{2\nu} \frac{\Gamma(1 + \nu_0 - \nu)\Gamma(1 - \nu_0 - \nu)}{\Gamma(1 + \nu)} \\ &\times \frac{\Gamma(1 - \nu)}{\Gamma(1 + \nu_0 + \nu)\Gamma(1 - \nu_0 + \nu)} \\ &\approx |\Delta|^{2\nu_0} \frac{\Gamma(1 - 2\nu_0)}{\Gamma(1 + \nu_0)} \frac{\Gamma(1 - \nu_0)}{\Gamma(1 + 2\nu_0)}. \end{aligned} \quad (\text{A20})$$

In the absence of the Efimov effect, ν_0 is real, as for a two-body problem with an angular momentum ℓ under $1/r^3$ potential $\nu_0 = 2\ell + 1$ [47, 62]. With the Efimov attraction, on the other hand, ν_0 becomes pure imaginary $\nu_0 = i|s|$. Therefore, \mathcal{M} at low energy is obtained as

$$\begin{aligned} \mathcal{M} &\cong |\Delta|^{2i|s|} \frac{-2\pi^2}{\sinh(\pi|s|)\sinh(2\pi|s|)} \frac{1}{[\Gamma(i|s|)\Gamma(1 + 2i|s|)]^2} \\ &= -|\Delta|^{2i|s|} e^{-2i\xi} = -e^{i\{2|s|\log|\Delta| - 2\xi\}}, \end{aligned} \quad (\text{A21})$$

where

$$\xi \equiv \arg[\Gamma(i|s|)\Gamma(1 + 2i|s|)]. \quad (\text{A22})$$

As shown in Eq. (A12), f^c decreases exponentially as $r \rightarrow 0$ while g^c increases exponentially, corresponding to a regular and irregular solution, respectively. If the length scale associated with the short-range physics R_{\min} is small $R_{\min} \ll \beta_3$, as is the case for cold atoms and molecules, the wave function should be solely described by the regular solution f^c . In other words, in the short-range region $r \ll \beta_3$, the potential is dominated by the repulsive $1/r^3$ interaction. Therefore, the wave function should be suppressed in the short-range region, which suggests

$$\begin{aligned} K^c &= \frac{1}{\sin[2\pi(\nu - \nu_0)]} \frac{1 - \mathcal{M}}{1 + \mathcal{M}} \\ &\cong 0 \quad \Delta \rightarrow 0. \end{aligned} \quad (\text{A23})$$

Namely,

$$\mathcal{M} \cong 1. \quad (\text{A24})$$

Substituting Eq. (A20) into this, we find

$$|s|\log|\Delta| - \xi = \left(-n + \frac{1}{2}\right)\pi, \quad (\text{A25})$$

from which we obtain the binding energy for a repulsive potential at low energy $|E| \ll 1/2\mu\beta_3^2$ as

$$|\Delta| = \exp\left\{\frac{1}{|s|}\left(\left(-n + \frac{1}{2}\right)\pi + \xi\right)\right\}. \quad (\text{A26})$$

2. Attractive case

The analytical solution of Eq. (1) for an attractive potential can also be obtained in a similar manner. Namely, the two independent solutions are defined as

$$\begin{aligned} f^c(r) &= \frac{1}{2\cos(\pi\nu)} \left[\frac{\xi(r)}{F(-\nu)} + \frac{\eta(r)}{F(\nu)} \right], \\ g^c(r) &= \frac{1}{2\sin(\pi\nu)} \left[\frac{\xi(r)}{F(-\nu)} - \frac{\eta(r)}{F(\nu)} \right]. \end{aligned} \quad (\text{A27})$$

Note that the definition of $c_n, Q(\nu), F(\nu)$ and the transcendental equation which determines ν are the same as those in the repulsive case. On the other hand, the equations between b_j and $c_j(\nu)$ are different from those in the repulsive case, and are given as [47],

$$b_j \equiv (-\Delta)^j \frac{\Gamma(\nu)\Gamma(\nu - \nu_0 + 1)\Gamma(\nu + \nu_0 + 1)}{\Gamma(\nu + j)\Gamma(\nu - \nu_0 + j + 1)\Gamma(\nu + \nu_0 + j + 1)} c_j(\nu), \quad (\text{A28})$$

$$b_{-j} \equiv (-\Delta)^j \frac{\Gamma(\nu - j + 1)\Gamma(\nu - \nu_0 - j)\Gamma(\nu + \nu_0 - j)}{\Gamma(\nu + 1)\Gamma(\nu - \nu_0)\Gamma(\nu + \nu_0)} c_j(-\nu), \quad (\text{A29})$$

With this slight difference in mind, a general solution for Eq. (1) is expressed by a linear combination of f^c and g^c as in Eq. (11).

The short-range asymptotic forms of Eq. (A27) for $r \ll \beta_3$ up to next-to-next-to-leading order can be obtained as

$$\begin{aligned} f^c(r) &\simeq \sqrt{\frac{r}{\pi}} \left(\frac{r}{\beta_3}\right)^{\frac{1}{4}} \left[1 - \frac{r}{2\beta_3} \left(|s|^2 + \frac{9}{16}\right) \left(|s|^2 + \frac{1}{16}\right) \right] \cos\Phi_r \\ &+ \sqrt{\frac{r}{\pi}} \left(\frac{r}{\beta_3}\right)^{\frac{3}{4}} \left(|s|^2 + \frac{1}{16}\right) \sin\Phi_r + O\left(\left(\frac{r}{\beta_3}\right)^{\frac{9}{4}}\right), \\ g^c(r) &\simeq -\sqrt{\frac{r}{\pi}} \left(\frac{r}{\beta_3}\right)^{\frac{1}{4}} \left[1 - \frac{r}{2\beta_3} \left(|s|^2 + \frac{9}{16}\right) \left(|s|^2 + \frac{1}{16}\right) \right] \sin\Phi_r \\ &+ \sqrt{\frac{r}{\pi}} \left(\frac{r}{\beta_3}\right)^{\frac{3}{4}} \left(|s|^2 + \frac{1}{16}\right) \cos\Phi_r + O\left(\left(\frac{r}{\beta_3}\right)^{\frac{9}{4}}\right). \end{aligned} \quad (\text{A30})$$

where $\Phi_r = 2\sqrt{\beta_3/r} - \pi/4$. The long-range asymptotic form in the attractive case is given by the same expression as in Eq. (A13) with $W_{f\pm}$ and $W_{g\pm}$ given as

$$\begin{aligned} W_{f-} &= \frac{1}{2\cos(\nu\pi)} \frac{1}{G(-\nu)} (1 + \mathcal{M}) \left(\sum_{m=-\infty}^{\infty} i^m b_m \right), \\ W_{f+} &= \frac{\tan(\nu\pi)}{2} \frac{1}{G(-\nu)} (1 - \mathcal{M}) \left(\sum_{m=-\infty}^{\infty} (-i)^m b_m \right), \\ W_{g-} &= \frac{1}{2\sin(\nu\pi)} \frac{1}{G(-\nu)} (1 - \mathcal{M}) \left(\sum_{m=-\infty}^{\infty} i^m b_m \right), \\ W_{g+} &= \frac{1}{2} \frac{1}{G(-\nu)} (1 + \mathcal{M}) \left(\sum_{m=-\infty}^{\infty} (-i)^m b_m \right), \end{aligned} \quad (\text{A31})$$

where the definitions of $G(\nu)$ and \mathcal{M} are the same as those in the repulsive case.

The binding energy can be obtained by introducing the boundary condition $\psi(r = \infty) = 0$ as

$$K^c = \frac{W_{f-}}{W_{g-}} = \tan(\nu\pi) \frac{1 + \mathcal{M}}{1 - \mathcal{M}}. \quad (\text{A32})$$

For an attractive potential, the right-hand side of Eq. (A32) at low energy regime can be approximated using Eqs. (A18), (A19) and (A20) (which are also valid for the attractive case) as

$$\frac{W_{f-}}{W_{g-}} \cong \tanh(\pi|s|) \tan \left[\frac{|s|}{2} \log |\Delta| - \xi \right]. \quad (\text{A33})$$

Substituting this into the bound-state condition Eq. (A32), the binding energy at low-energy regime $|E| \ll 1/2\mu\beta_3^2$ is obtained as

$$|\Delta| = \exp \left(\frac{1}{|s|} \left[\arctan \left(\frac{K^c}{\tanh(\pi|s|)} \right) + \xi \right] \right) \times e^{-\frac{\pi\pi}{|s|}}. \quad (\text{A34})$$

For an attractive case, the three-body binding energy depends explicitly on the QDT parameter K^c .

To determine the QDT parameter K^c , a boundary condition at short range region is needed. In this study, we adopt the hard-wall boundary condition $\psi(r = R_{\min}) = 0$, from which K^c is obtained as

$$\begin{aligned} K^c &= -\tanh(\pi|s|) \frac{\operatorname{Re} \left[J_{2i|s|} \left(2\sqrt{\frac{\beta_3}{R_{\min}}} \right) \right]}{\operatorname{Im} \left[J_{2i|s|} \left(2\sqrt{\frac{\beta_3}{R_{\min}}} \right) \right]} \\ &\cong -\frac{1}{\tan \left[2\sqrt{\frac{\beta_3}{R_{\min}}} - \frac{\pi}{4} \right]}. \end{aligned} \quad (\text{A35})$$

In the last line, $R_{\min} \ll \beta_3$ is assumed to obtain the asymptotic form of K^c . Notably, K^c for small R_{\min} is independent of energy nor s , which is consistent with the s -insensitive (i.e. angular-momentum-insensitive) quantum defect theory used in our study [59].

Appendix B: Zero-energy solution

To clarify the relations between the zero-energy solutions Eqs. (17) and (21) and the finite-energy solutions Eqs. (A1) and (A27), we present here the derivation of the zero-energy solutions by taking the zero-energy limit of the finite-energy solutions.

1. Repulsive case

First, we derive the zero-energy solutions Eq. (17) in the repulsive case. From Eq. (A2), $\xi(r)$ in Eq. (A1) is

reformulated as

$$\begin{aligned} \xi(r) &= \sqrt{r} \sum_{m=-\infty}^{m=\infty} b_m J_{\nu+m}(x) \\ &= \sqrt{r} \sum_{m=-\infty}^{m=\infty} \sum_{s=0}^{s=\infty} b_m \frac{(-1)^s}{s! \Gamma(s + \nu + m + 1)} \left(\frac{x}{2} \right)^{2s+\nu+m} \\ &= \sqrt{r} \sum_{m=-\infty}^{m=\infty} \sum_{s=0}^{s=\infty} b_{-m-2s} \frac{(-1)^s}{s! \Gamma(\nu - m - s + 1)} \left(\frac{x}{2} \right)^{\nu-m}. \end{aligned} \quad (\text{B1})$$

In the last line, m is replaced by $-m - 2s$. Introducing $y \equiv 2\sqrt{\beta_3}/r$, (i.e., $x = 8\Delta/y^2$), we obtain

$$\begin{aligned} \xi(r) &= \sqrt{r} \sum_{m=-\infty}^{m=\infty} \sum_{s=0}^{s=\infty} b_{-m-2s} \frac{(-1)^s}{s! \Gamma(\nu - m - s + 1)} \left(\frac{4\Delta}{y^2} \right)^{\nu-m} \\ &= \sqrt{r} \left(\frac{y}{2} \right)^{-2\nu} \sum_{m=-\infty}^{m=\infty} p_m \left(\frac{y}{2} \right)^{2m}, \end{aligned} \quad (\text{B2})$$

where p_m is defined as Eq. (A15) in Ref. [62]

$$p_m \equiv \Delta^\nu \sum_{s=0}^{s=\infty} \frac{(-1)^s \Delta^{2s}}{s! \Gamma(\nu - m - s + 1)} \Delta^{-(m+2s)} b_{-m-2s}. \quad (\text{B3})$$

At low-energy $|\Delta| \ll 1$, large m terms in $\xi(r)$ are dominant and p_m can be replaced with $\lim_{m \rightarrow \infty} p_m$. As shown in Eq. (A16) in Ref. [62], the limit of large m of p_m is given as

$$\lim_{m \rightarrow \infty} p_m = F(-\nu) \frac{1}{m! \Gamma(-2\nu + m + 1)}. \quad (\text{B4})$$

Replacing p_m in Eq. (B2) with $\lim_{m \rightarrow \infty} p_m$, we obtain the zero-energy limit of $\xi(r)$ as

$$\begin{aligned} \lim_{E \rightarrow 0} \xi(r) &= \sqrt{r} F(-\nu_0) \sum_{m=-\infty}^{m=\infty} \frac{1}{m! \Gamma(-2\nu_0 + m + 1)} \left(\frac{y}{2} \right)^{2m-2\nu_0} \\ &= \sqrt{r} F(-\nu_0) I_{-2\nu_0} \left(2\sqrt{\frac{\beta_3}{r}} \right), \end{aligned} \quad (\text{B5})$$

where the low-energy property $\nu \simeq \nu_0 = s$ is used in the first line.

Similarly, the zero-energy limit of $\eta(r)$ is obtained as

$$\lim_{E \rightarrow 0} \eta(r) = \sqrt{r} F(\nu_0) I_{2\nu_0} \left(2\sqrt{\frac{\beta_3}{r}} \right). \quad (\text{B6})$$

Then, from Eq. (A1), we obtain the zero-energy limits of f^c and g^c as

$$\begin{aligned} \lim_{E \rightarrow 0} f^c(r) &= -\frac{2}{\sinh(2\pi|s|)} \operatorname{Im} \left[\sqrt{r} I_{2i|s|} \left(2\sqrt{\frac{\beta_3}{r}} \right) \right], \\ \lim_{E \rightarrow 0} g^c(r) &= -2\operatorname{Re} \left[\sqrt{r} I_{2i|s|} \left(2\sqrt{\frac{\beta_3}{r}} \right) \right]. \end{aligned} \quad (\text{B7})$$

2. Attractive case

The zero-energy solution in the attractive case [Eq. (21)] is obtained in a similar manner as in the repulsive case. Following the same procedure as Eq. (B2), $\xi(r)$ is reformulated as

$$\xi(r) = \sqrt{r} \left(\frac{y}{2}\right)^{-2\nu} \sum_{m=-\infty}^{m=\infty} p_m \left(\frac{y}{2}\right)^{2m}, \quad (\text{B8})$$

where p_m is given as Eq. (B3). Taking into account the difference of the definition of b_n between the repulsive and attractive cases, $\lim_{m \rightarrow \infty} p_m$ is given as

$$\lim_{m \rightarrow \infty} p_m = F(-\nu) \frac{(-1)^m}{m! \Gamma(-2\nu + m + 1)}. \quad (\text{B9})$$

[1] I. Bloch, J. Dalibard, and W. Zwerger, Many-body physics with ultracold gases, *Rev. Mod. Phys.* **80**, 885 (2008).

[2] F. Schäfer, T. Fukuhara, S. Sugawa, Y. Takasu, and Y. Takahashi, Tools for quantum simulation with ultracold atoms in optical lattices, *Nature Reviews Physics* **2**, 411 (2020).

[3] S. L. Cornish, M. R. Tarbutt, and K. R. Hazzard, Quantum computation and quantum simulation with ultracold molecules, *Nature Physics* **20**, 730 (2024).

[4] T. Kraemer, M. Mark, P. Waldburger, J. G. Danzl, C. Chin, B. Engeser, A. D. Lange, K. Pilch, A. Jaakkola, H. C. Nägerl, and R. Grimm, Evidence for Efimov quantum states in an ultracold gas of Cesium atoms, *Nature* **440**, 315 (2006).

[5] V. Efimov, Energy levels arising from resonant two-body forces in a three-body system, *Phys. Lett. B* **33**, 563 (1970).

[6] V. Efimov, Energy levels of three resonantly interacting particles, *Nucl. Phys. A* **210**, 157 (1973).

[7] C. H. Greene, P. Giannakeas, and J. Pérez-Ríos, Universal few-body physics and cluster formation, *Rev. Mod. Phys.* **89**, 035006 (2017).

[8] P. Naidon and S. Endo, Efimov physics: a review, *Rep. Prog. Phys.* **80**, 056001 (2017).

[9] J. P. D'Incao, Few-body physics in resonantly interacting ultracold quantum gases, *J. Phys. B* **51**, 043001 (2018).

[10] S. Inouye, M. R. Andrews, J. Stenger, H. J. Miesner, D. M. Stamper-Kurn, and W. Ketterle, Observation of Feshbach resonances in a Bose-Einstein condensate, *Nature* **392**, 151 (1998).

[11] C. Chin, R. Grimm, P. Julienne, and E. Tiesinga, Feshbach resonances in ultracold gases, *Rev. Mod. Phys.* **82**, 1225 (2010).

[12] R. Briihl, A. Kalinin, O. Kornilov, J. P. Toennies, G. C. Hegerfeldt, and M. Stoll, Matter wave diffraction from an inclined transmission grating: Searching for the elusive ${}^4\text{He}$ trimer Efimov state, *Phys. Rev. Lett.* **95**, 063002 (2005).

[13] M. Kunitski, S. Zeller, J. Voigtsberger, A. Kalinin, L. P. H. Schmidt, M. Schöffler, A. Czasch, W. Schöllkopf, R. E. Grisenti, T. Jahnke, et al., Observation of the Efimov state of the helium trimer, *Science* **348**, 551 (2015).

[14] Y. Nishida, Y. Kato, and C. D. Batista, Efimov effect in quantum magnets, *Nature Physics* **9**, 93 (2013).

[15] H. W. Hammer and L. Platter, Efimov states in nuclear and particle physics, *Ann. Rev. Nucl. Part. Sci.* **60**, 207 (2010).

[16] S. Endo, E. Epelbaum, P. Naidon, Y. Nishida, K. Sekiguchi, and Y. Takahashi, Three-body forces and Efimov physics in nuclei and atoms, *Eur. Phys. J. A* **61**, 9 (2025).

[17] I. Tanihata, M. Alcorta, D. Bandyopadhyay, R. Bieri, L. Buchmann, B. Davids, N. Galinski, D. Howell, W. Mills, S. Mythili, R. Openshaw, E. Padilla-Rodal, G. Ruprecht, G. Sheffer, A. C. Shotter, M. Trinczek, P. Walden, H. Savajols, T. Roger, M. Caamano, W. Mittig, P. Roussel-Chomaz, R. Kanungo, A. Gallant, M. Notani, G. Savard, and I. J. Thompson, Measurement of the two-halo neutron transfer reac-

Replacing p_m in Eq. (B8) with $\lim_{m \rightarrow \infty} p_m$, we obtain the zero-energy limit of $\xi(r)$ as

$$\begin{aligned} \lim_{E \rightarrow 0} \xi(r) &= \sqrt{r} F(-\nu_0) \sum_{m=-\infty}^{m=\infty} \frac{(-1)^m}{m! \Gamma(-2\nu_0 + m + 1)} \left(\frac{y}{2}\right)^{2m-2\nu_0} \\ &= \sqrt{r} F(-\nu_0) J_{-2\nu_0} \left(2\sqrt{\frac{\beta_3}{r}}\right), \end{aligned} \quad (\text{B10})$$

where the low-energy property $\nu \simeq \nu_0 = s$ is used in the first line.

Similarly, the zero-energy limit of $\eta(r)$ is obtained as

$$\lim_{E \rightarrow 0} \eta(r) = \sqrt{r} F(\nu_0) J_{2\nu_0} \left(2\sqrt{\frac{\beta_3}{r}}\right). \quad (\text{B11})$$

Then, from Eq. (A27), we obtain the zero-energy limits of f^c and g^c as

$$\begin{aligned} \lim_{E \rightarrow 0} f^c(r) &= \frac{1}{\cosh(\pi|s|)} \text{Re} \left[\sqrt{r} J_{2i|s|} \left(2\sqrt{\frac{\beta_3}{r}}\right) \right], \\ \lim_{E \rightarrow 0} g^c(r) &= -\frac{1}{\sinh(\pi|s|)} \text{Im} \left[\sqrt{r} J_{2i|s|} \left(2\sqrt{\frac{\beta_3}{r}}\right) \right]. \end{aligned} \quad (\text{B12})$$

tion $^1\text{H}(^{11}\text{Li}, ^9\text{Li})^3\text{H}$ at $3a$ MeV, Phys. Rev. Lett. **100**, 192502 (2008).

[18] R. Higa, H.-W. Hammer, and U. Van Kolck, $\alpha\alpha$ scattering in halo effective field theory, Nucl. Phys. A **809**, 171 (2008).

[19] D. Hove, E. Garrido, P. Sarriguren, D. V. Fedorov, H. O. U. Fynbo, A. S. Jensen, and N. T. Zinner, Emergence of clusters: Halos, Efimov states, and experimental signals, Phys. Rev. Lett. **120**, 052502 (2018).

[20] S. Endo and J. Tanaka, Efimov states in excited nuclear halos, arXiv:2309.04131 (2023).

[21] M. Zaccanti, B. Deissler, C. D'Errico, M. Fattori, M. Jona-Lasinio, S. Müller, G. Roati, M. Inguscio, and G. Modugno, Observation of an Efimov spectrum in an atomic system, Nature Physics **5**, 586 (2009).

[22] N. Gross, Z. Shotan, S. Kokkelmans, and L. Khaykovich, Observation of universality in ultracold ^7Li three-body recombination, Phys. Rev. Lett. **103**, 163202 (2009).

[23] S. E. Pollack, D. Dries, and R. G. Hulet, Universality in three- and four-body bound states of ultracold atoms, Science **326**, 1683 (2009).

[24] S.-K. Tung, K. Jiménez-García, J. Johansen, C. V. Parker, and C. Chin, Geometric scaling of Efimov states in a $^6\text{Li}-^{133}\text{Cs}$ mixture, Phys. Rev. Lett. **113**, 240402 (2014).

[25] R. Pires, J. Ulmanis, S. Häfner, M. Repp, A. Arias, E. D. Kuhnle, and M. Weidemüller, Observation of Efimov resonances in a mixture with extreme mass imbalance, Phys. Rev. Lett. **112**, 250404 (2014).

[26] S. A. Moses, J. P. Covey, M. T. Miecnikowski, D. S. Jin, and J. Ye, New frontiers for quantum gases of polar molecules, Nature Physics **13**, 13 (2017).

[27] L. Chomaz, I. Ferrier-Barbut, F. Ferlaino, B. Laburthe-Tolra, B. L. Lev, and T. Pfau, Dipolar physics: a review of experiments with magnetic quantum gases, Rep. Prog. Phys. **86**, 026401 (2022).

[28] F. Böttcher, J.-N. Schmidt, M. Wenzel, J. Hertkorn, M. Guo, T. Langen, and T. Pfau, Transient supersolid properties in an array of dipolar quantum droplets, Phys. Rev. X **9**, 011051 (2019).

[29] L. Tanzi, E. Lucioni, F. Famà, J. Catani, A. Fioretti, C. Gabbanini, R. N. Bisset, L. Santos, and G. Modugno, Observation of a dipolar quantum gas with metastable supersolid properties, Phys. Rev. Lett. **122**, 130405 (2019).

[30] L. Chomaz, D. Petter, P. Ilzhöfer, G. Natale, A. Trautmann, C. Politi, G. Durastante, R. M. W. van Bijnen, A. Patscheider, M. Sohmen, M. J. Mark, and F. Ferlaino, Long-lived and transient supersolid behaviors in dipolar quantum gases, Phys. Rev. X **9**, 021012 (2019).

[31] Y. Kawaguchi, H. Saito, and M. Ueda, Einstein-de Haas effect in dipolar Bose-Einstein condensates, Phys. Rev. Lett. **96**, 080405 (2006).

[32] H. Matsui, Y. Miyazawa, R. Goto, C. Nakano, Y. Kawaguchi, M. Ueda, and M. Kozuma, Observation of the Einstein-de Haas effect in a Bose-Einstein condensate, Science **391**, 384 (2026).

[33] A. Micheli, G. K. Brennen, and P. Zoller, A toolbox for lattice-spin models with polar molecules, Nature Physics **2**, 341 (2006).

[34] A. N. Carroll, H. Hirzler, C. Miller, D. Wellnitz, S. R. Muleady, J. Lin, K. P. Zamarski, R. R. W. Wang, J. L. Bohn, A. M. Rey, and J. Ye, Observation of generalized $t - J$ spin dynamics with tunable dipolar interactions, Science **388**, 381 (2025).

[35] J.-R. Li, K. Matsuda, C. Miller, A. N. Carroll, W. G. Tobias, J. S. Higgins, and J. Ye, Tunable itinerant spin dynamics with polar molecules, Nature **614**, 70 (2023).

[36] K.-K. Ni, S. Ospelkaus, D. Wang, G. Quéméner, B. Neyenhuis, M. De Miranda, J. Bohn, J. Ye, and D. Jin, Dipolar collisions of polar molecules in the quantum regime, Nature **464**, 1324 (2010).

[37] S. Ospelkaus, K.-K. Ni, D. Wang, M. De Miranda, B. Neyenhuis, G. Quéméner, P. Julienne, J. Bohn, D. Jin, and J. Ye, Quantum-state controlled chemical reactions of ultracold potassium-rubidium molecules, Science **327**, 853 (2010).

[38] M. Guo, B. Zhu, B. Lu, X. Ye, F. Wang, R. Vexiau, N. Bouloufa-Maafa, G. Quéméner, O. Dulieu, and D. Wang, Creation of an ultracold gas of ground-state dipolar $^{23}\text{Na}-^{87}\text{Rb}$ molecules, Phys. Rev. Lett. **116**, 205303 (2016).

[39] T. Karman, M. Tomza, and J. Pérez-Ríos, Ultracold chemistry as a testbed for few-body physics, Nature Physics **20**, 722 (2024).

[40] K. Matsuda, L. De Marco, J.-R. Li, W. G. Tobias, G. Valtolina, G. Quéméner, and J. Ye, Resonant collisional shielding of reactive molecules using electric fields, Science **370**, 1324 (2020).

[41] L. Anderegg, S. Burchesky, Y. Bao, S. S. Yu, T. Karman, E. Chae, K.-K. Ni, W. Ketterle, and J. M. Doyle, Observation of microwave shielding of ultracold molecules, Science **373**, 779 (2021).

[42] D. DeMille, Quantum computation with trapped polar molecules, Phys. Rev. Lett. **88**, 067901 (2002).

[43] L. R. Picard, A. J. Park, G. E. Patenotte, S. Gebretsadkan, D. Wellnitz, A. M. Rey, and K.-K. Ni, Entanglement and iSWAP gate between molecular qubits, Nature **637**, 821 (2025).

[44] E. P. Wigner, On the behavior of cross sections near thresholds, Phys. Rev. **73**, 1002 (1948).

[45] L. D. Landau and E. M. Lifshitz, Quantum mechanics: non-relativistic theory, Vol. 3 (Pergamon Press, 1977).

[46] J. Bohn, M. Cavagnaro, and C. Ticknor, Quasi-universal dipolar scattering in cold and ultracold gases, New J. Phys. **11**, 055039 (2009).

[47] B. Deb and L. You, Low-energy atomic collision with dipole interactions, Phys. Rev. A **64**, 022717 (2001).

[48] K. Kanjilal and D. Blume, Low-energy resonances and bound states of aligned bosonic and fermionic dipoles, Phys. Rev. A **78**, 040703 (2008).

[49] Y. Wang, J. P. D'Incao, and C. H. Greene, Efimov effect for three interacting bosonic dipoles, Phys. Rev. Lett. **106**, 233201 (2011).

[50] Y. Wang, J. P. D'Incao, and C. H. Greene, Universal three-body physics for fermionic dipoles, Phys. Rev. Lett. **107**, 233201 (2011).

[51] M. Berninger, A. Zenesini, B. Huang, W. Harm, H. C. Nägerl, F. Ferlaino, R. Grimm, P. S. Julienne, and J. M. Hutson, Universality of the three-body parameter for Efimov states in ultracold Cesium, Phys. Rev. Lett. **107**, 120401 (2011).

[52] N. Gross, Z. Shotan, O. Machtey, S. Kokkelmans, and L. Khaykovich, Study of Efimov physics in two nuclear-spin sublevels of ^7Li , Compt. Rend. Phys. **12**, 4 (2011).

[53] P. Naidon, S. Endo, and M. Ueda, Physical origin of

the universal three-body parameter in atomic Efimov physics, *Phys. Rev. A* **90**, 022106 (2014).

[54] P. Naidon, S. Endo, and M. Ueda, Microscopic origin and universality classes of the Efimov three-body parameter, *Phys. Rev. Lett.* **112**, 105301 (2014).

[55] J. Wang, J. P. D’Incao, B. D. Esry, and C. H. Greene, Origin of the three-body parameter universality in Efimov physics, *Phys. Rev. Lett.* **108**, 263001 (2012).

[56] Y. Wang, J. Wang, J. P. D’Incao, and C. H. Greene, Universal three-body parameter in heteronuclear atomic systems, *Phys. Rev. Lett.* **109**, 243201 (2012).

[57] S. Häfner, J. Ulmanis, E. D. Kuhnle, Y. Wang, C. H. Greene, and M. Weidemüller, Role of the intraspecies scattering length in the Efimov scenario with large mass difference, *Phys. Rev. A* **95**, 062708 (2017).

[58] B. Gao, Solutions of the Schrödinger equation for an attractive $1/r^6$ potential, *Phys. Rev. A* **58**, 1728 (1998).

[59] B. Gao, Angular-momentum-insensitive quantum-defect theory for diatomic systems, *Phys. Rev. A* **64**, 010701 (2001).

[60] B. Gao, Binding energy and scattering length for diatomic systems, *J. Phys. B* **37**, 4273 (2004).

[61] B. Gao, General form of the quantum-defect theory for $-1/r^\alpha$ type of potentials with $\alpha > 2$, *Phys. Rev. A* **78**, 012702 (2008).

[62] B. Gao, Repulsive $1/r^3$ interaction, *Phys. Rev. A* **59**, 2778 (1999).

[63] J. Jie, S. Chen, Y. Chen, and R. Qi, Exact solutions and quantum defect theory for van der Waals potentials in ultracold molecular systems, *J. Phys. B* **58**, 175201 (2025).

[64] R. Du, Analytical solutions of the Schrödinger equation for two confined particles with the van der Waals interaction, *Few-Body Systems* **65**, 98 (2024).

[65] R. Du, R. Qi, and P. Zhang, Solutions of the Schrödinger equation for anisotropic dipole-dipole interaction plus van der Waals interaction, *Phys. Rev. Res.* **7**, 023162 (2025).

[66] B. Gao, E. Tiesinga, C. J. Williams, and P. S. Julienne, Multichannel quantum-defect theory for slow atomic collisions, *Phys. Rev. A* **72**, 042719 (2005).

[67] J. F. E. Croft, A. O. G. Wallis, J. M. Hutson, and P. S. Julienne, Multichannel quantum defect theory for cold molecular collisions, *Phys. Rev. A* **84**, 042703 (2011).

[68] K. Oi, P. Naidon, and S. Endo, Universality of Efimov states in highly mass-imbalanced cold-atom mixtures with van der Waals and dipole interactions, *Phys. Rev. A* **110**, 033305 (2024).

[69] Y. Nishida and S. Tan, Liberating Efimov physics from three dimensions, *Few-Body Systems* **51**, 191 (2011).

[70] G. Lamporesi, J. Catani, G. Barontini, Y. Nishida, M. Inguscio, and F. Minardi, Scattering in mixed dimensions with ultracold gases, *Phys. Rev. Lett.* **104**, 153202 (2010).

[71] A. V. Avdeenkov, M. Kajita, and J. L. Bohn, Suppression of inelastic collisions of polar $^1\Sigma$ state molecules in an electrostatic field, *Phys. Rev. A* **73**, 022707 (2006).

[72] T. Shi, H. Wang, and X. Cui, Universal bound states with Bose-Fermi duality in microwave-shielded polar molecules, arXiv preprint arXiv:2504.21535 (2025).

[73] J. Stuhler, A. Griesmaier, T. Koch, M. Fattori, T. Pfau, S. Giovanazzi, P. Pedri, and L. Santos, Observation of dipole-dipole interaction in a degenerate quantum gas, *Phys. Rev. Lett.* **95**, 150406 (2005).

[74] K. Aikawa, A. Frisch, M. Mark, S. Baier, A. Rietzler, R. Grimm, and F. Ferlaino, Bose-Einstein condensation of Erbium, *Phys. Rev. Lett.* **108**, 210401 (2012).

[75] M. Lu, N. Q. Burdick, S. H. Youn, and B. L. Lev, Strongly dipolar Bose-Einstein condensate of dysprosium, *Phys. Rev. Lett.* **107**, 190401 (2011).

[76] H. A. Bethe and R. Peierls, The scattering of neutrons by protons, *Proc. Roy. Soc. London A* **149**, 176 (1935).

[77] A. C. Fonseca, E. F. Redish, and P. Shanley, Efimov effect in an analytically solvable model, *Nucl. Phys. A* **320**, 273 (1979).

[78] S. Sinha and L. Santos, Cold dipolar gases in quasi-one-dimensional geometries, *Phys. Rev. Lett.* **99**, 140406 (2007).

[79] F. Deuretzbacher, J. C. Cremon, and S. M. Reimann, Ground-state properties of few dipolar bosons in a quasi-one-dimensional harmonic trap, *Phys. Rev. A* **81**, 063616 (2010).

[80] F. Schäfer, N. Mizukami, and Y. Takahashi, Feshbach resonances of large-mass-imbalance Er-Li mixtures, *Phys. Rev. A* **105**, 012816 (2022).

[81] F. Schäfer, Y. Haruna, and Y. Takahashi, Observation of Feshbach resonances in an ^{167}Er - ^6Li Fermi-Fermi mixture, *J. Phys. Soc. Jpn.* **92**, 054301 (2023).

[82] K. Xie, X. Li, Y.-Y. Zhou, J.-H. Luo, S. Wang, Y.-Z. Nie, H.-C. Shen, Y.-A. Chen, X.-C. Yao, and J.-W. Pan, Feshbach spectroscopy of ultracold mixtures of ^6Li and ^{164}Dy atoms, *Phys. Rev. A* **111**, 023327 (2025).

[83] A. Ciamei, S. Finelli, A. Trenkwalder, M. Inguscio, A. Simoni, and M. Zaccanti, Exploring ultracold collisions in ^6Li - ^{53}Cr Fermi mixtures: Feshbach resonances and scattering properties of a novel alkali-transition metal system, *Phys. Rev. Lett.* **129**, 093402 (2022).

[84] H. Yang, J. Cao, Z. Su, J. Rui, B. Zhao, and J.-W. Pan, Creation of an ultracold gas of triatomic molecules from an atom-diatom molecule mixture, *Science* **378**, 1009 (2022).

[85] H. Yang, D.-C. Zhang, L. Liu, Y.-X. Liu, J. Nan, B. Zhao, and J.-W. Pan, Observation of magnetically tunable feshbach resonances in ultracold ^{23}Na - ^{40}K + ^{40}K collisions, *Science* **363**, 261 (2019).

[86] X.-Y. Chen, A. Schindewolf, S. Eppelt, R. Bause, M. Duda, S. Biswas, T. Karman, T. Hilker, I. Bloch, and X.-Y. Luo, Field-linked resonances of polar molecules, *Nature* **614**, 59 (2023).

[87] Y. He, Z. Chen, H. Zhen, M. Huang, M. K. Parit, and G.-B. Jo, Exploring the Berezinskii-Kosterlitz-Thouless transition in a two-dimensional dipolar bose gas, *Science Advances* **11**, eadrl2715 (2025).

[88] S. Roy, M. Landini, A. Trenkwalder, G. Semeghini, G. Spagnolli, A. Simoni, M. Fattori, M. Inguscio, and G. Modugno, Test of the universality of the three-body Efimov parameter at narrow Feshbach resonances, *Phys. Rev. Lett.* **111**, 053202 (2013).

[89] R. Chapurin, X. Xie, M. J. Van de Graaff, J. S. Popowski, J. P. D’Incao, P. S. Julienne, J. Ye, and E. A. Cornell, Precision test of the limits to universality in few-body physics, *Phys. Rev. Lett.* **123**, 233402 (2019).

[90] X. Xie, M. J. Van de Graaff, R. Chapurin, M. D. Frye, J. M. Hutson, J. P. D’Incao, P. S. Julienne, J. Ye, and E. A. Cornell, Observation of Efimov universality across a non-universal Feshbach resonance in ^{39}K , *Phys. Rev. Lett.* **125**, 243401 (2020).

[91] J. Johansen, B. DeSalvo, K. Patel, and C. Chin, Testing

universality of Efimov physics across broad and narrow Feshbach resonances, *Nature Physics* **13**, 731 (2017).

[92] T. Secker, D. J. M. Ahmed-Braun, P. M. A. Mestrom, and S. J. J. M. F. Kokkelmans, Multichannel effects in the Efimov regime from broad to narrow Feshbach resonances, *Phys. Rev. A* **103**, 052805 (2021).

[93] D. S. Petrov, Three-boson problem near a narrow Feshbach resonance, *Phys. Rev. Lett.* **93**, 143201 (2004).

[94] A. O. Gogolin, C. Mora, and R. Egger, Analytical solution of the bosonic three-body problem, *Phys. Rev. Lett.* **100**, 140404 (2008).

[95] P. K. Sørensen, D. V. Fedorov, A. S. Jensen, and N. T. Zinner, Efimov physics and the three-body parameter within a two-channel framework, *Phys. Rev. A* **86**, 052516 (2012).

[96] J. van de Kraats, D. J. M. Ahmed-Braun, J.-L. Li, and S. J. J. M. F. Kokkelmans, Efimovian three-body potential from broad to narrow Feshbach resonances, *Phys. Rev. A* **107**, 023301 (2023).

[97] J. van de Kraats, D. J. M. Ahmed-Braun, J.-L. Li, and S. J. J. M. F. Kokkelmans, Emergent inflation of the Efimov spectrum under three-body spin-exchange interactions, *Phys. Rev. Lett.* **132**, 133402 (2024).

[98] K. Oi and S. Endo, Universal Efimov spectra and fermionic doublets in highly mass-imbalanced cold-atom mixtures with van der Waals and dipole interactions, *Phys. Rev. Res.* **7**, 033236 (2025).

[99] Y. Tang, W. Kao, K.-Y. Li, S. Seo, K. Mallayya, M. Rigol, S. Gopalakrishnan, and B. L. Lev, Thermalization near integrability in a dipolar quantum newton's cradle, *Phys. Rev. X* **8**, 021030 (2018).

[100] W. Kao, K.-Y. Li, K.-Y. Lin, S. Gopalakrishnan, and B. L. Lev, Topological pumping of a 1d dipolar gas into strongly correlated prethermal states, *Science* **371**, 296 (2021).

[101] K. Wang, C. P. Williams, L. R. Picard, N. Y. Yao, and K.-K. Ni, Enriching the quantum toolbox of ultracold molecules with Rydberg atoms, *PRX Quantum* **3**, 030339 (2022).

[102] L. Guan, X. Cui, R. Qi, and H. Zhai, Quasi-one-dimensional dipolar quantum gases, *Phys. Rev. A* **89**, 023604 (2014).

[103] M. Zdziennicki, M. Ślusarczyk, K. Pawłowski, and K. Jachymski, Effective interactions in quasi-one-dimensional dipolar quantum gases, *Phys. Rev. A* **112**, 063318 (2025).

[104] T. Bergeman, M. G. Moore, and M. Olshanii, Atom-atom scattering under cylindrical harmonic confinement: Numerical and analytic studies of the confinement induced resonance, *Phys. Rev. Lett.* **91**, 163201 (2003).

[105] T. Lompe, T. B. Ottenstein, F. Serwane, A. N. Wenz, G. Zürn, and S. Jochim, Radio-frequency association of Efimov trimers, *Science* **330**, 940 (2010).

[106] S. Nakajima, M. Horikoshi, T. Mukaiyama, P. Naidon, and M. Ueda, Measurement of an Efimov trimer binding energy in a three-component mixture of ${}^6\text{Li}$, *Phys. Rev. Lett.* **106**, 143201 (2011).

[107] O. Machtey, Z. Shotan, N. Gross, and L. Khaykovich, Association of Efimov trimers from a three-atom continuum, *Phys. Rev. Lett.* **108**, 210406 (2012).

[108] Y. Yudkin, R. Elbaz, P. Giannakeas, C. H. Greene, and L. Khaykovich, Coherent superposition of Feshbach dimers and Efimov trimers, *Phys. Rev. Lett.* **122**, 200402 (2019).

[109] F. Werner and X. Leyronas, Three-body contact for fermions. I. General relations, *Compt. Rend. Phys.* **25**, 179 (2024).

[110] E. Braaten, D. Kang, and L. Platter, Universal relations for identical bosons from three-body physics, *Phys. Rev. Lett.* **106**, 153005 (2011).

[111] R. J. Fletcher, R. Lopes, J. Man, N. Navon, R. P. Smith, M. W. Zwierlein, and Z. Hadzibabic, Two- and three-body contacts in the unitary Bose gas, *Science* **355**, 377 (2017).